Materials Science and Engineering C 33 (2013) 663–667

Contents lists available at SciVerse ScienceDirect

Materials Science and Engineering C

journal homepage: www.elsevier.com/locate/msec

A facile preparation route for netlike microstructures on a stainless steel using an ethanol-mediated femtosecond laser irradiation

Hao Bian, Qing Yang, Hewei Liu, Feng Chen *, Guangqing Du, Jinhai Si, Xun Hou

State Key Laboratory for Manufacturing Systems Engineering & Key Laboratory of Photonics Technology for Information, School of Electronics & Information Engineering, Xi'an Jiaotong University, Xianing-xilu 28, Xi'an 710049, China

ARTICLE INFO

Article history:
Received 31 July 2012
Received in revised form 25 September 2012
Accepted 26 October 2012
Available online 2 November 2012

Keywords:
Femtosecond laser
Microstructures
Self-assembly
Surface modification

ABSTRACT

Netlike or porous microstructures are highly desirable in metal implants and biomedical monitoring applications. However, realization of such microstructures remains technically challenging. Here, we report a facile and environmentally friendly method to prepare netlike microstructures on a stainless steel by taking the full advantage of the liquid-mediated femtosecond laser ablation. An unordered netlike structure and a quasi-ordered array of holes can be fabricated on the surface of stainless steel via an ethanol-mediated femtosecond laser line-scan method. SEM analysis of the surface morphology indicates that the porous netlike structure is in the micrometer scale and the diameter of the quasi-ordered holes ranges from 280 nm to 320 nm. Besides, we find that the obtained structures are tunable by altering the laser processing parameters especially scanning speed.

1. Introduction

Netlike or porous structures on metals with spatial resolutions in the submicrometer or nanometer scale have received significant attention in material fields over the past decades because of their unique properties associated with potential applications in biomedical monitoring, metal implants, optical devices and superhydrophobic materials [1–4]. Thus, many groups concentrated on the fabrication of porous nanostructures in the past decades. Reviewing previous works, approaches to prepare such structures mainly include anodic oxidation [5], chemical treatment [6], ion beam etching and plasma-spray [7,8]. Up to now, it still evokes considerable research interest to develop an efficient and environmentally benign method to prepare porous and netlike structures. And these structures have a broad prospect of applications in biomedical devices, especially for those surface-modified metallic implants [9,10].

Therefore, developing a simple and effective fabrication technique for nano-texturing of metals is a vigorous scientific research field recently. Because of its advantages as a single-step and environmentally benign process, laser-induced periodic surface structures (LIPSS) open up an attractive approach for surface-texturing of metals. Since the 1960s, almost at the time when lasers came out, the periodic microgrooves or so-called classic ripples were found after the laser irradiated the solid surfaces. However, the feature size of these classic ripples is in the micrometer scale, which cannot satisfy the demands of nanoscale fabrication.

In recent years, femtosecond laser is successfully established to be an excellent tool to produce fine nanostructures on various solid materials, such as metals, dielectrics, semiconductors and polymers. The feature size of the femtosecond laser-induced periodic surface structures (FLIPSS) can be reduced to less than 100 nm. Nevertheless, typical femtosecond laser-induced structures reported in the literature had a few limitations such as nanospikes, random roughness, subwavelength ripple microprotrusions and holes [11–17].

Random nanostructures, like spikes or particles, are usually obtained at low fluence or single-shot irradiations. Ripples or grating pattern is the most common FLIPSS which is produced at intermediate fluences. In a normal case, the interspacing of the ripples (Λ) follows the equation:

$$\Lambda = \lambda/n, \tag{1}$$

where λ is the laser wavelength and n is the refractive index of the materials, and the orientation is perpendicular to the laser polarization. For high-fluence irradiation, the surface structures are produced in the micrometer scale, such as microprotrusions and holes. The formation of the aforementioned surface structures involves various processes including the inference, surface plasma waves (SPW), self-organization, melting and resolidification and capillary waves, but which of these processes dominates the formation mechanism is still an open question. Although the morphology, mechanisms and applications of the metallic FLIPSS were widely studied in the past, we notice that most experiments concentrated on the FLIPSS of metals produced in air. Herein, we perform our studies on the metallic FLIPSS produced in ethanol, and interestingly, some novel surface structures are observed. These types of structures will increase the surface area of materials and have good applications in numerous scientific fields.

* Corresponding author. Tel./fax: +86 29 82668420.
E-mail address: chenfeng@mail.xjtu.edu.cn (F. Chen).

0928-4931/$ – see front matter © 2012 Elsevier B.V. All rights reserved.
http://dx.doi.org/10.1016/j.msec.2012.10.014

In this letter, we reveal our findings on the fabrication of various nano-scaled netlike and porous structures on a stainless steel by a femtosecond laser in ambient ethanol. Then, we show that the surface structures are closely related to the laser fluence and laser scanning speed. For example, uniform netlike and porous structures are produced when the laser fluence $F = 0.45$ J/cm^2. In air, however, the typical nanogratings are produced at the same incident laser fluences. Finally, the mechanisms of the morphological discrepancies between ethanol and air ambience are discussed.

2. Experimental

2.1. Experimental setup

The laser source was a Ti:sapphire oscillator–amplifier system (FEMTOPOWER Compact Pro, FEMTOLASERS), which delivered 800 nm, 30 fs Gaussian laser pulses at a repetition rate of 1 kHz. The laser pulses were focused via a 10× microscope objective lens (Nikon, N.A. = 0.3) and the corresponding diameter of the focal spot was about 3.3 μm. The energy of the incident laser could be continuously varied by metallic neutral density filters, and the laser power was measured by a pyroelectric detector. The number of pulses delivered to the sample was controlled by an electromechanical shutter. The sample was stuck to the bottom of a 10 ml glass container which was mounted on a computer-controlled three-axis stage (M-505.2DG, Physik Instrumente). When the glass container was filled up with liquid, the thickness of the liquid layer above the sample surface was about 5 mm. The sample was just placed on the focal point of the objective lens. Observation of the fabrication processing was accomplished by a tungsten lamp light source and a CCD camera with a video monitor. The obtained microstructure of the sample is observed by a field-emission scanning electronic microscope (FE-SEM, JEOL JSM-7000F).

2.2. Preparation of samples

The sample used in our experiment was an AISI 304 stainless steel (Baoji, China) which was cut into a bulk with dimensions of $10 \times 10 \times 5$ mm^3. Before femtosecond-pulsed laser treatment, the surface was mechanically polished and cleaned by an ultrasonic bath in acetone for 15 min and rinsed in ethanol. After the laser experiment, the sample was cleaned by ultrasonic bath in ethanol for 15 min.

2.3. Scanning path

To achieve large-area fabrication of micro- and nanostructures on the stainless steel, the laser pulses were scanned line-by-line on the sample surface. In the experiment, 50 scan-lines with a length of 100 μm and interspacing of 2 μm were used to create 100×100 μm^2 irradiated regions.

3. Results and discussion

We initially investigate the evolution of femtosecond-laser-induced micro/nanostructures in different media via comparing multi-shot irradiations on the steel bulk. The experiments were carried out in air, deionized water and absolute ethanol (analytical pure, 99.9%, Tianjin Fuyuhg Company). Multi-shot irradiations were produced by femtosecond laser with N = 100, 500, 1000 pulses at a pulse energy of $F = 0.55$ J cm^{-2}.

Fig. 1 displays a scanning electron microscope (SEM) image of the multi-shot irradiated regions produced in ambient air (Fig. 1(a)–(c)), deionized water (Fig. 1(d)–(f)) and ethanol (Fig. 2(g)–(i)). The pulse energy F of the incident laser was 1.5 μJ and the number of shots N was 100, 500 and 1000, respectively. Typical ripples with spacing of 550 nm appear in irradiated regions in air experiment with $N = 100$ (Fig. 1(a)) and 500 (Fig. 1(b)) but vanish in 5000-shots irradiation.

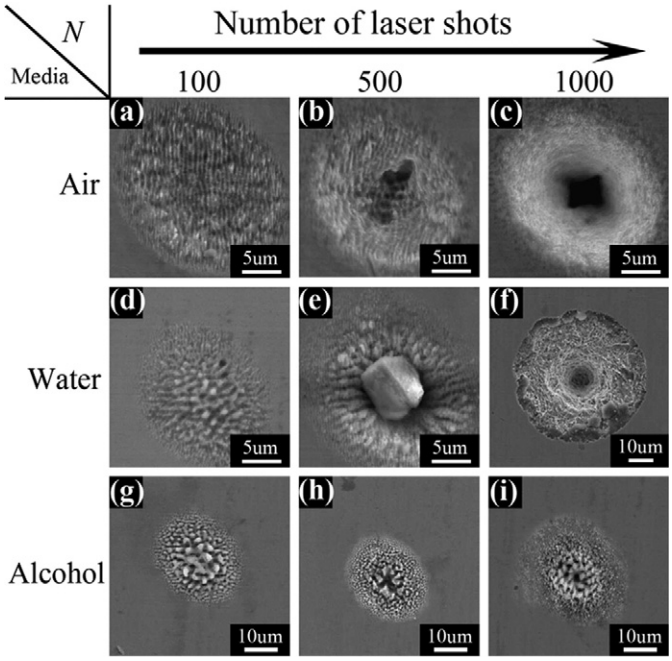

Fig. 1. Femtosecond laser multi-shot irradiations produced in air (a–c), deionized water (d–f) and ethanol (g–i). The used pulse energy is 0.55 J cm^{-2} and number of pulses are N = 100, 500, 1000.

This is because femtosecond laser ablation occurred in the 5000-shot irradiation damaging the ripple patterns, and ablation appeared. The presence of water disturbed the formation of uniform ripple patterns, inducing ripple-covered random microstructures (Fig. 1(d) and (e)) and microroughness (Fig. 1(f)). For ethanol-mediated irradiation, the laser-induced structures are dissimilar to those created in air or water. We found that various distinct types of structures with characteristic sizes ranging from nanometers to micrometers distribute regularly in the irradiated regions.

Fig. 2 shows the scanning electron microscope (SEM) images of the porous structures induced in ambient ethanol on the stainless steel. In the experiment, an intermediated laser influence $F = 0.55$ J cm^{-2} was employed to avoid excessive ablation and thermal damage of materials. From the figures, we can see that the typical ripple patterns were not obtained. For high scanning speed ($V = 320$ μm s^{-1}), a quasi-ordered array of holes with smooth surfaces was induced, as shown in Fig. 2(a) and (b). The unconnected holes exhibit elliptical or circular shapes and distributed in the laser-irradiated region with the density of around 6×10^8 per cm^2. The size of each hole ranges from 280 nm to 320 nm. When the scanning speed, V, was slowed down to 20 μm s^{-1}, a uniform porous netlike structure with rough surfaces appears (Fig. 2(c) and (d)). The inset of Fig. 2(d) shows that nanorods, with a diameter of about 100–200 nm and a length of about 1–2 μm, self-assembled on the sample, leading to the formation of such loose and rough surfaces. Furthermore, the individual pores shown in Fig. 2(d), with sizes ranging from nanometers to micrometers, are interconnected.

Interestingly, the typical ripple structures were successfully induced in an air environment with the same laser fluences and scanning speeds, as demonstrated in Fig. 3. Actually, we failed to create similar porous or netlike structures whether in single-spot irradiation (showed in Fig. 3(a) and (b)) or in line-scan mode (showed in Fig. 3(c)), and these netlike microstructures formed only in the ethanol environment. It should be noted that the two types of porous structures obtained in our experiment are similar to those closed-cell porous metals (quasi-ordered hole array) and open-cell porous metals (uniform netlike structure), which are widely used as metal implants. The loose structures on the metal surfaces would reduce the Young's moduli of

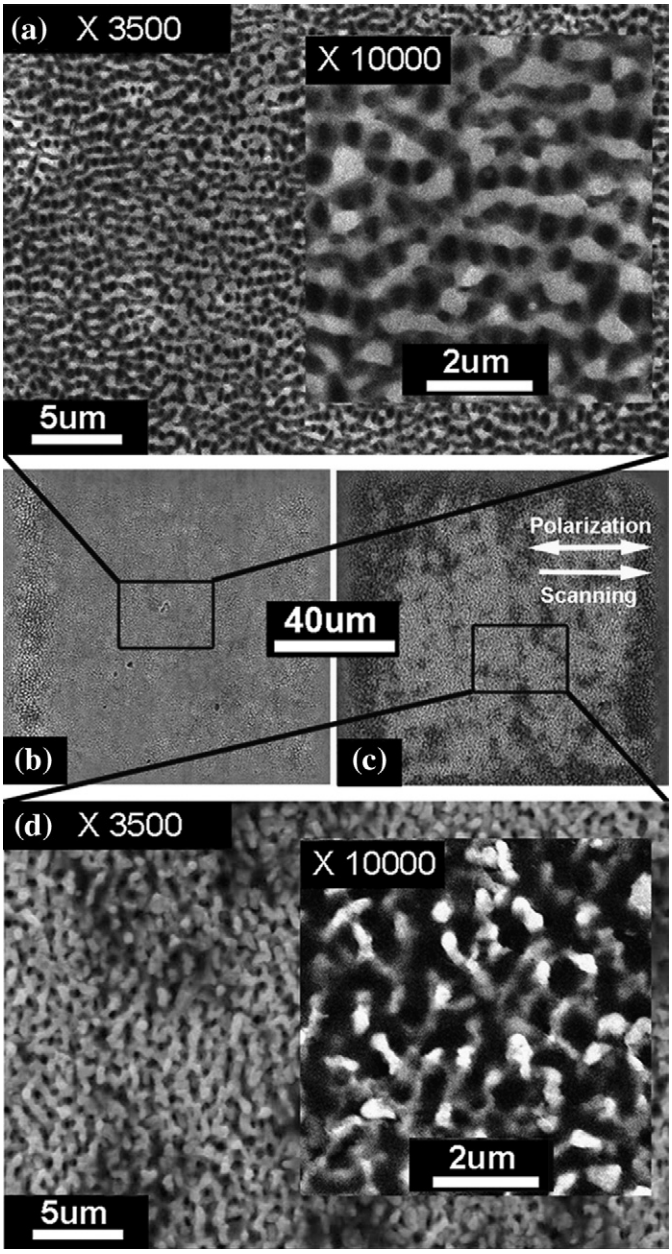

Fig. 2. Femtosecond laser induced the quasi-ordered array of holes (a, b) and unordered netlike structure (c, d) on the stainless steel. The laser fluence is $F = 0.55$ J cm^{-2}. The scanning speeds are $V = 320$ μm s^{-1} for (a, b) and 20 μm s^{-1} for (c, d).

the implants close to the surrounding human bones and pores proved to be beneficial to osseointegration [18]. Compared to the chemical treatments for the fabrication of porous structures, femtosecond laser processing is environmentally benign and free from surface contaminations.

To elucidate the formation of the porous surface structures, we textured the samples by changing the processing parameters. The evolution of the surface structures as a function of scanning speed is presented in Fig. 4. The alteration of the surface structures induced by the laser irradiation is related to the scanning speed because it will influence the number of shots deposited in a unit area. For rapid scanning speeds, e. g. $V = 320$ μm s^{-1}, the quasi-ordered hole array formed in the irradiated region (Fig. 2(a)). Further SEM investigation suggests that this porous pattern can be divided into a series of belt-like units with orientations approximately parallel to the scanning direction, as shown in Fig. 4(a). In addition, grating-like structures can be observed in each individual belt-like unit. The grating-like structures with a period from 270 nm to 340 nm which is about 40% of the laser wavelength are perpendicular to the laser polarization, which are exactly consistent with the features of the ripples or grating-like structures. For femtosecond laser–matter interactions, a universal phenomenon is the appearance of the subwavelength grating-like structures in whole irradiated regions. The formation mechanism is thought to be associated with the periodic distribution of the laser fluence, which resulted from the interference of incident laser pulses and excited surface plasma waves [19]. Consequently, the sample surfaces are selectively photoetched and the grating-like structure (ripples) is printed on the surfaces with the period (Λ):

$$\Lambda = \lambda/2n \tag{2}$$

where λ is the wavelength of the laser; and n is the refractive index of the material for normal incidence [20]. However, the formation of the hole array refers to a much more complex nature of the laser-irradiated liquid/solid interface because the laser fluence used in the experiment can easily evoke various liquid-related effects, such as the generation of bubbles and non-linear optical effects [21]. These effects would last for a relatively long period of time and interact with the incoming pulses, leading to the inhomogeneous distribution of the laser fluence. Thus, the interference process is localized and occurs separately in each belt-like region and consequently, the quasi-ordered hole array is formed, as shown in Fig. 2(a). The selective etch at the liquid/solid interface was also observed by R. Böhme et al., who obtained a concentric annulus pattern on fused silica using an ultrashort laser single-spot irradiation [22]. In our experiment, we used the line-scan mode and the etched regions are approximately parallel to the scanning direction.

If the scanning speed is slowed down, the number of shots per unit area will increase. At intermediated speed (e.g. $V = 80$ μm s^{-1}), an island-protrusion structure formed, as shown in Fig. 4(b). The protrusions at micrometer scale were also found during the femtosecond and picosecond laser ablation of metals in liquids [23–26]. Unlike the grating-like structures, the interplay of the thermal melting and mechanical-pressures plays a dominate role in the formation of the uniform protrusion patterns. As aforementioned, holes and craters were generated by relatively small amount of laser shots; when the pulse number increased, residual energy of the subsequent pulses would be concentrated in the formed craters or holes, resulting in

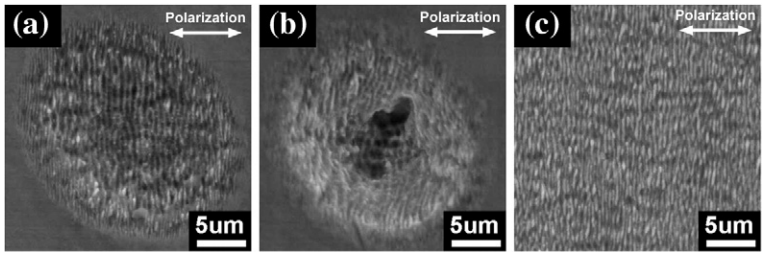

Fig. 3. Grating-like structures (ripples) induced by femtosecond laser in ambient air. (a) 100-shot crater at $F = 0.55$ J cm^{-2}; (b) 100-shot crater at $F = 0.98$ J cm^{-2}; (c) large-area ripples induced by line-scan method, $F = 0.55$ J cm^{-2}, $V = 320$ μm s^{-1}.

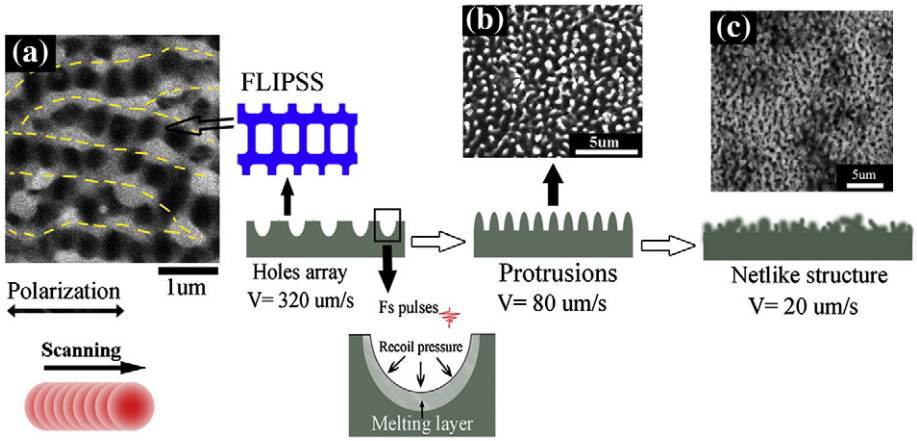

Fig. 4. Schematic diagram: evolution of the surface structures as a function of scanning speed. (a) SEM image of the quasi-ordered array of holes. Dashed lines divide the pattern into a variety of belt-like units. (b) SEM image of the micro-protrusions. (c) SEM image of the netlike microstructures.

surface melting inside the holes. Meanwhile, the laser pulses could evaporate the ethanol layer near the focal point and shockwaves and mechanical forces are inevitably generated. Therefore, the liquid-related recoil pressures would push the melted materials out of the holes and craters, which will be re-solidified by the surrounding liquid and form the protrusions. It is reported that the solidification process under the confinement of liquids is much longer than in air or gas environments [27], which is essential to the complex remodeling of the metallic surface structures. At $V = 20\ \mu m\ s^{-1}$, repeat melting and resolidification processes of materials, cooperated with the liquid-related mechanical pressures, enable us to fabricate the netlike surface structures on stainless steel successfully.

Subsequently, the influence of surface structures on the laser fluences was studied. We failed to fabricate any porous or netlike structures on the sample surface when the laser fluences were higher than 1.28 J cm^{-2}, but unstable microrough surfaces were obtained. This is because the residual thermal effects occur during femtosecond laser ablation of materials at high laser fluences [28]. Following the laser ablation, a fraction of absorbed laser energy is retained in the heat-affected zone. This absorbed energy further dissipates into the bulk of the sample and remains as residual thermal energy which induces the bulk temperature of the sample to rise. Thermal melting and laser-induced shockwaves would damage the micro- and nanostructures, generating such unstable microrough surfaces. The experimental results indicate that the porous structures in the micro- or nanometer scales can only be prepared when the laser fluence is relatively low; besides, the morphological characteristics of the formed structures can also be controlled via altering the scanning speed.

What is more, the similar surface microstructures were also observed by a nanosecond laser–matter interaction in the semiconfined configuration [29–31]. Generally, the mechanism of fs laser–matter interaction related to the interaction of photons with electrons. The thermal transfer between the lattices is ignored because of the short duration of femtosecond laser and the metal melting does not occur in femtosecond laser irradiation. This is quite different from the nanosecond laser–matter interaction. In the ambient ethanol, the femtosecond laser can easily evoke various liquid-related effects, such as the generation of bubbles and non-linear optical effects [32]. The ethanol not only cools down the sample and removes the ejections, but it also participates in the laser–matter interaction such as forming the porous structures. This is quite different from the nanoholes generated by nanosecond laser in the semiconfined configuration [30]. Their origin is conjectured from the generation of solitary waves in the target plasma by the piston effect. In the semiconfined configuration, the solitary waves humps as the plasma density waves interact with the target surface, thus leaving the thermal/pressure fingerprints in the form of nanoholes.

It is worth mentioning that the femtosecond laser fabrication of porous and netlike surface structures can be extended to other metals. For example, we have obtained similar structures on titanium, titanium alloy (Ti_6Al_4V) and aluminum. Furthermore, to reduce the processing time, the structures were prepared in regions with dimensions of $100 \times 100\ \mu m^2$. However, it is quite simple for us to fabricate the structures in much larger areas.

4. Conclusions

In summary, by the ethanol-mediated irradiations with a femtosecond laser, quasi-ordered hole array and porous netlike micro-/nanostructures were fabricated on the metal surface. These structures are quite different from the grating-like structure or ripples obtained in femtosecond laser-irradiated regions in ambient air. The morphological characteristics of the structures are tunable by altering the scanning speed and the laser fluence. The evolution and formation of the structures involve complex laser–liquid-material mechanisms, such as interference of incident laser and SPW, liquid-induced uniform distribution of laser fluence, prolonged melting and resolidification process and mechanical pressure remodeling process.

Acknowledgments

This work was supported by the National Science Foundation of China under the grant no. 61176113 and the Fundamental Research Funds for the Central Universities.

References

[1] H.M. Kim, F. Miyaji, T. Kokubo, T. Nakamura, J. Biomed. Mater. Res. 32 (1996) 409–417.
[2] Q. Yu, P. Guan, D. Qin, G. Golden, P.M. Wallace, Nano Lett. 8 (2008) 1923–1928.
[3] D.F.P. Pile, D.K. Gramotnev, Opt. Lett. 29 (2004) 1069–1071.
[4] W.L. Barnes, A. Dereux, T.W. Ebbesen, Nature 424 (2003) 824–830.
[5] R.C. Furneaux, W.R. Rigby, A.P. Aavidson, Nature 337 (1989) 147–149.
[6] O. Jessensky, F. Müller, U. Gösele, Appl. Phys. Lett. 72 (1998) 1173–1175.
[7] T.W. Ebbesen, H.J. Lezec, H.F. Ghaemi, T. Thio, P.A. Wolff, Nature 391 (1998) 667–669.
[8] A. Gaggl, G. Schultes, W.D. Müller, H. Kärcher, Biomaterials 21 (2000) 1067–1073.
[9] N. Sykaras, A.M. Iacopino, V.A. Marker, R.G. Triplett, R.D. Woody, Int. J. Oral Maxillofac. Implants 15 (2000) 675–690.
[10] J.E. Davies, Int. J. Prosthodont. 11 (1998) 391–401.
[11] Quan-Zhong Zhao, Stefan Malzer, Li-Jun Wang, Opt. Express 24 (2007) 15741–15746.
[12] A.Y. Vorobyev, Guo Chunlei, Opt. Express 6 (2006) 2164–2169.
[13] L. Qi, K. Nishii, Y. Namba, Opt. Lett. 12 (2009) 1846–1848.
[14] Q.Z. Zhao, S. Malzer, L.J. Wang, Opt. Lett. 32 (2007) 1932–1934.
[15] A.Y. Vorobyev, C. Guo, J. Appl. Phys. 104 (2008) (063523-063523-3).
[16] V. Oliveira, S. Ausset, R. Vilar, Appl. Surf. Sci. 255 (2009) 7556–7560.
[17] Y. Yang, J. Yang, C. Liang, H. Wang, X. Zhu, N. Zhang, Opt. Express 23 (2009) 21124–21133.

[18] G. Ryan, A. Pandit, D.P. Apatsidis, Biomaterials 27 (2006) 2651–2670.
[19] S. Sakabe, M. Hashida, S. Tokita, S. Namba, K. Okamuro, Phys. Rev. B 79 (2009) (033409-1-4).
[20] T.Q. Jia, F.L. Zhao, M. Huang, H.X. Chen, J.R. Qiu, R.X. Li, Z.Z. Xu, H. Kuroda, Appl. Phys. Lett. 88 (2006).
[21] C. Spielmann, N.H. Burnett, S. Sartania, R. Koppitsch, M. Schnurer, C. Kan, M. Lenzner, P. Wobrauschek, F. Krausz, Science 278 (1997) 661–664.
[22] R. Böhme, C. Vass, B. Hopp, K. Zimmer, Nanotechnology 19 (2008) 495301.
[23] E. Stratakis, V. Zorba, M. Barberoglou, C. Fotakis, G.A. Shafeev, Appl. Surf. Sci. 255 (2009) 5346–5350.
[24] E. Stratakis, V. Zorba, M. Barberoglou, C. Fotakis, G.A. Shafeev, Nanotechnology 20 (10) (2009) 105303–105311.
[25] E.V. Zavedeev, A.V. Petrovskaya, A.V. Simakin, G.A. Shafeev, Quantum Electron. 36 (2006) 978–980.
[26] S. Lau Truong, G. Levi, F. Bozon-Verduraz, A.V. Petrovskaya, A.V. Simakin, G.A. Shafeev, Appl. Phys. A 89 (2007) 373–376.
[27] W.W. Gong, Z.H. Zheng, J.J. Zheng, H.F. Zhao, X.G. Ren, S.Z. Lu, Appl. Surf. Sci. 255 (2009) 4351–4354.
[28] A.Y. Vorobyev, V.M. Kuzmichev, N.G. Kokody, P. Kohns, J. Dai, C. Guo, Appl. Phys. A 82 (2006) 357–362.
[29] S. Lugomer, B. Mihaljević, G. Peto, A. Toth, E. Horvath, J. Appl. Phys. 97 (2005) 073305.
[30] S. Lugomer, A. Maksimovic, G. Peto, A. Toth, E. Horvath, J. Appl. Phys. 100 (2006) 104308.
[31] S. Lugomer, A. Maksimovic, A. Karacs, G. Peto, Appl. Surf. Sci. 257 (2011) 7851–7855.
[32] H. Liu, F. Chen, X. Wang, Q. Yang, H. Bian, J. Si, X. Hou, Thin Solid Films 518 (2010) 5188–5194.